

## **Appendix K.**

# **Microbial Respiration in Bottom Waters**

This appendix contains a comparison of observed and predicted water column oxygen-consuming processes in the bottom waters of the Salish Sea.

### **ADA Accessibility**

This appendix may contain tables, graphics, and images that may not meet accessibility standards. The Department of Ecology is committed to providing people with disabilities access to information and services by meeting or exceeding the requirements of the Americans with Disabilities Act (ADA), Sections 504 and 508 of the Rehabilitation Act, and Washington State Policy #188. To request an ADA accommodation, contact the Environmental Assessment Program Publications Coordinator at [EAPPubs@ecy.wa.gov](mailto:EAPPubs@ecy.wa.gov) or call 564-669-3028. For Washington Relay Service or TTY call 711 or 877-833-6341. Visit [Ecology's website](#) for more information.<sup>1</sup>

---

<sup>1</sup><https://ecology.wa.gov/about-us/accessibility-equity/accessibility>

# Table of Contents

	Page
<b>Microbial Respiration Processes and Their Predictions</b> .....	<b>2</b>
Observational dataset.....	5
<b>Analytical Approach</b> .....	<b>9</b>
<b>Results</b> .....	<b>10</b>
<b>Conclusions</b> .....	<b>16</b>
<b>References</b> .....	<b>17</b>

# Microbial Respiration Processes and Their Predictions

A key process in marine environments is respiration, mediated by autotrophic or heterotrophic microorganisms via the breakdown and metabolism of organic material. Respiration consumes oxygen and produces carbon dioxide. Micro-heterotrophs can comprise a significant portion of respiratory activity in coastal waters (Williams 1981). The Salish Sea Model (SSM) predicts both microalgal respiration and micro-heterotrophic respiration.

Microalgal respiration is modeled as a component of algal basal metabolism within the Integrated Compartment Model (ICM), the biogeochemical model used in SSM. Basal metabolism increases with temperature, and the fraction of respiration in the total basal metabolism is regulated by the amount of oxygen present in the water column. Respiration is a lower fraction of the total when oxygen levels are low. Heterotrophic microbial respiration is simulated as the dissolution of organic carbon in the water column via first-order kinetics (Cerco and Cole 1995). Globally specified base heterotrophic rates are adjusted during the model simulation in every grid cell according to changing temperatures, organic carbon concentrations, and dissolved oxygen (DO) levels. The units used to represent microbial respiration rates are mass/volume/time.

SSM can simulate and track processes that consume dissolved oxygen, including respiration, on an individual basis. In our simulations, processes are output as DDOC for heterotrophic respiration and NITRIF for the nitrification occurring in the water column. Those two processes, along with algal respiration, cover the oxygen-consuming processes we simulated in the water column. RESP is comprised of the sum of autotrophic and heterotrophic respiration (DDOC) as well as nitrification (NITRIF). We compute algal respiration by subtracting DDOC and NITRIF from RESP, and we label it ALG\_RESP.

Spatial distributions of the maxima, minima, and mean predictions of RESP for the bottom layer are shown in the planview maps for 2006 and 2014 in Figure K-1. Note the difference in the scales. The pattern of overall respiration is similar in both years. Terminal inlets and bays are predicted to have higher respiration rates. Maximum rates of respiration are predicted to occur at the tips of inlets, particularly in South Sound and Skagit Bay. Minimum rates of respiration are predicted at the tip of Lynch Cove, located at the end of the Great Bend of Hood Canal. Low oxygen levels in bottom layers at this location can occur year-round and likely limit the minimal respiration rates predicted there.

The temporal variation of predictions is represented in Figure K-2, which shows the variation of RESP at a single site in Bellingham Bay by month of the year based on four SSM runs for the years 2000, 2006, 2008, and 2014. The months with the largest predicted variations in respiration rate are March and April. July and September exhibit the peak predicted rates, while February is the lowest at this site. Figure K-3 shows the proportion of each of the oxygen-consuming processes mentioned above, predicted by month, over the same years, at sites that correspond to respiration observational sites shown in Figure K-4. Algal respiration in the early spring, summer, and early fall months is proportionally greater than in the winter and late fall months. Heterotrophic respiration is predicted to be proportionally greater in the winter

(January – February) at these sites, whereas nitrification is predicted to be slightly greater in December.

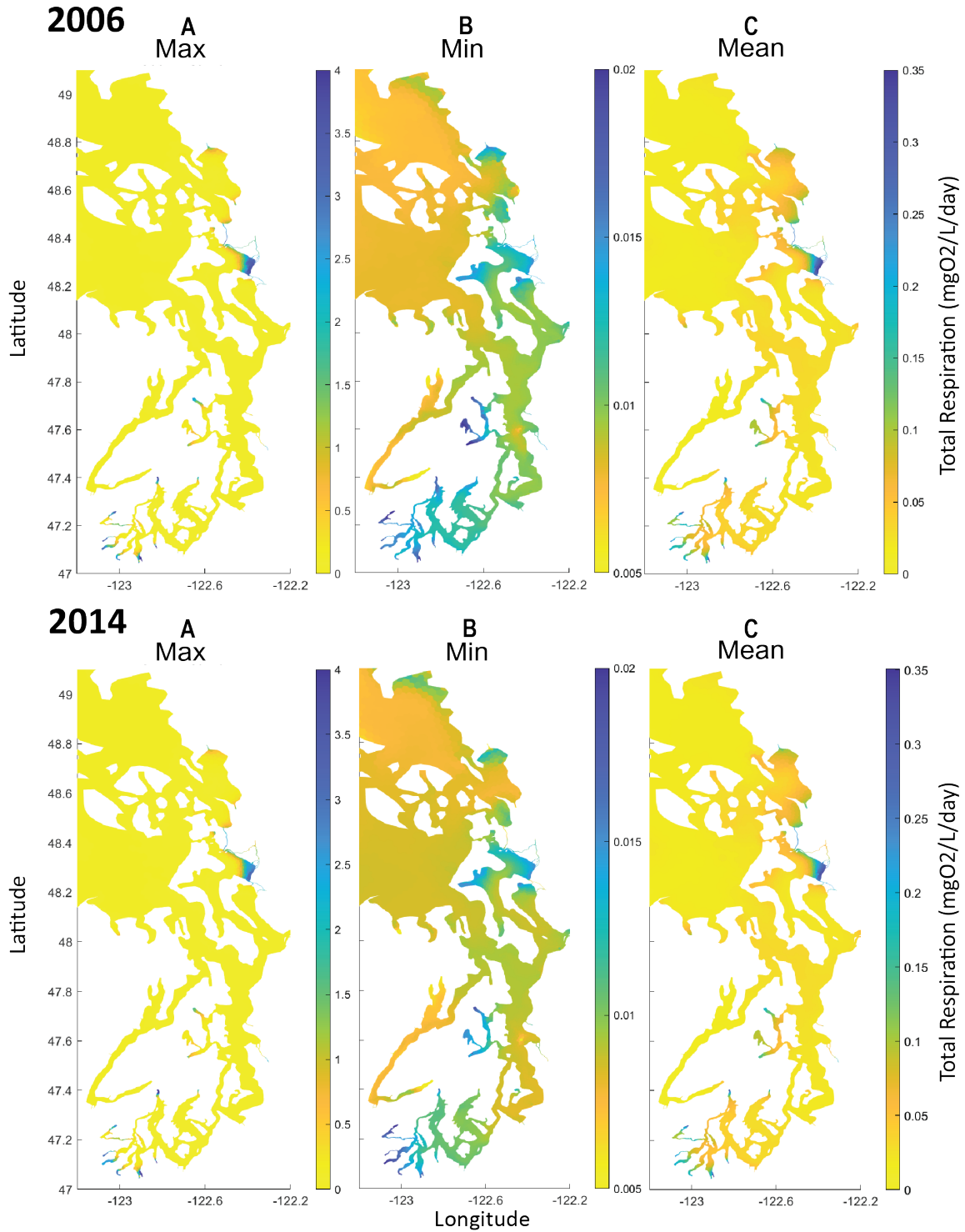


**Figure K-1. Planview maps of Predicted Total Respiration in the Bottom Layer for 2006 and 2014.**

Shown are the maxima (A), minima (B), and mean(C) in units of mg O<sub>2</sub>/L/day.

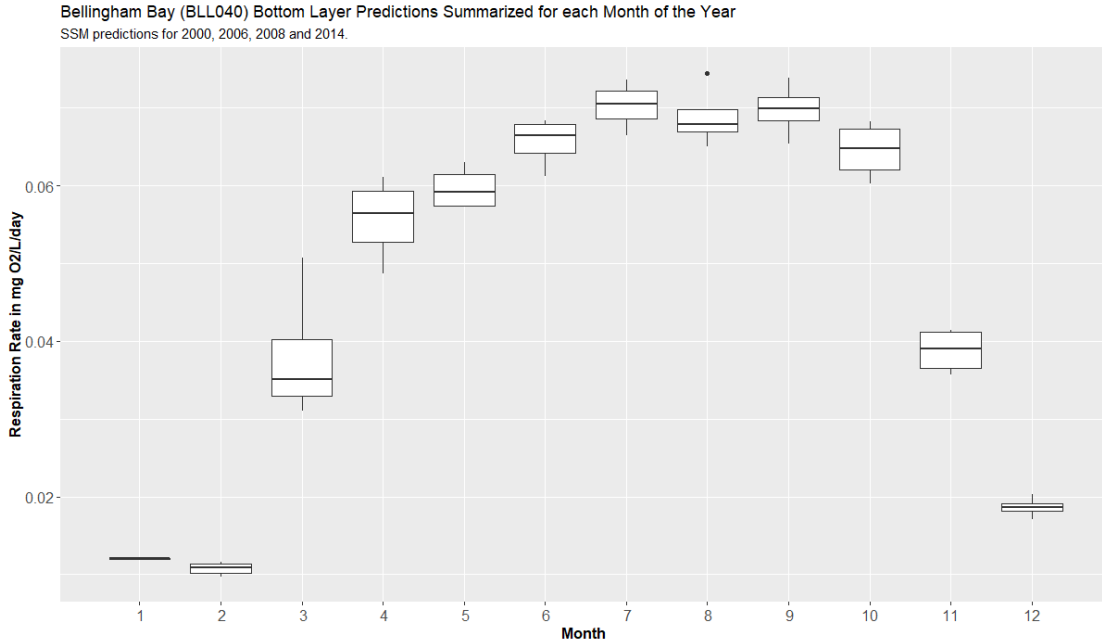


**Figure K-2. Monthly Boxplots of Predicted Total Respiration at BLL040 in Bottom Site: Bellingham Bay. Years predicted are 2000, 2006, 2008, and 2014. Units are mg O<sub>2</sub>/L/day.**

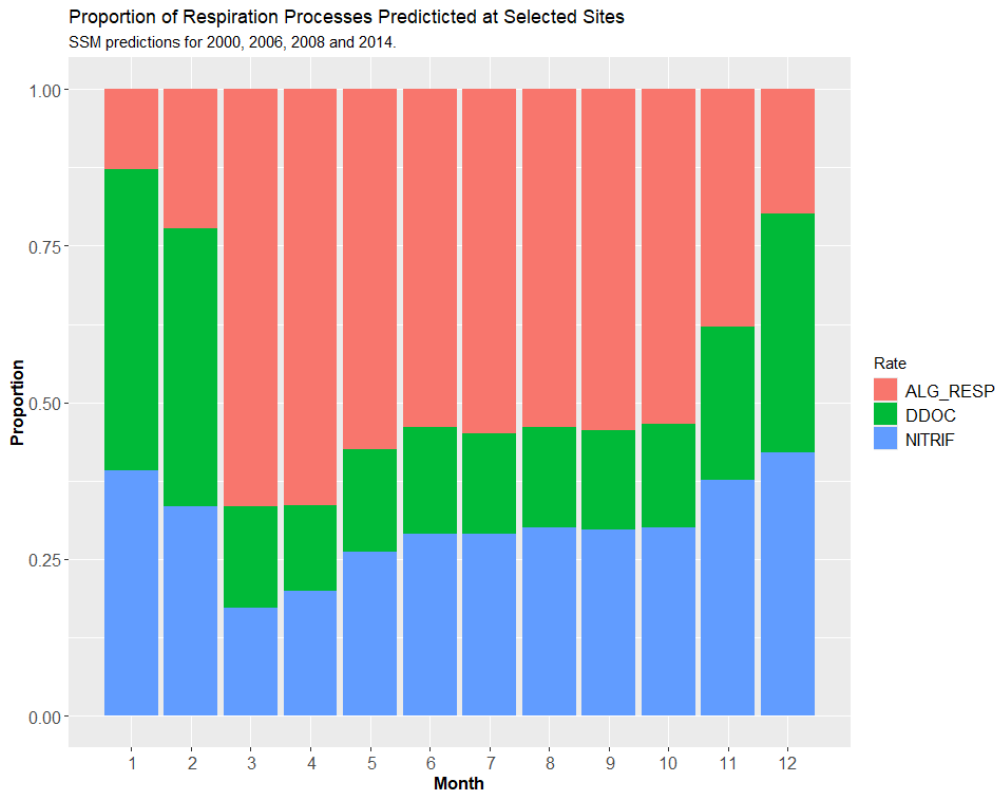


**Figure K-3. Predicted Proportion of Oxygen Consuming Processes in the Bottom Layer at Selected Sites.**

Algal respiration is shown in pink, heterotrophic respiration in green, and nitrification in blue.

## Observational dataset

We are aware of only one observational study of microbial respiration rate measurements encompassing multiple sites throughout the U.S. portion of the Salish Sea. Apple et al. (2019) described procedures for sampling and analysis of microbial respiration within the Salish Sea.

Near-bottom water samples (within 0.5 meters of the sediment) were collected from September 2018 to October 2019 in 2L Niskin bottles from 15 sites and transported to Padilla Bay National Estuarine Research Reserve Laboratory, where incubations were conducted. Each sample was separated into four sub-samples for which the decrease in oxygen concentration was measured 2 – 6 times a day for at least 21 days. Figure K-4 shows the locations of the microbial respiration sites. While laboratory replicates were routinely produced by dividing samples obtained from each location into up to four replicate samples for incubation, it was only feasible to obtain field replicates at one location (BLL040).



**Figure K-4. Map of Microbial Respiration Sites.**  
(Apple et al. 2019).

The microbial respiration data are publicly accessible via the Washington State Department of Ecology’s Environmental Information Management System (EIM). The link to the data is cited within the Apple and Bjornson (2019) reference. Observations are not available for January.

Bottom water conditions during sample collection covered a range of temperatures, dissolved oxygen concentrations, and salinities. Means for each site are shown in Table K-1. The minimum temperature was 7.2°C at BLL040 in March, and the maximum was 18.3°C at Oakland

Bay (OAK004), the shallowest site observed, in September. Dissolved oxygen ranged from concentrations of 3.6 mg/L at PSS019 in January to 11.3 mg/L at DNA001 in March. Salinities ranged from 22 psu at SKG003 in December and January to 36.3 psu in GOR001 and CRR001 in November.

Apple and Bjornson incubated all samples in the dark at a target temperature of 10°C. Antia (1976) published studies on the survival of 37 microplanktonic algal species kept in darkness at 10°C and other temperatures. Strains kept at temperatures like those that the algae were accustomed to survived longer at those temperatures. The most resistant survivors were benthic types, out of which 70% tolerated 11 – 12 months of darkness and the rest at least 5-6 months of darkness. Given the ability of algal strains to live in darkness for so long, we assume that algae collected by Apple and Bjornson (2019) remained present in the samples throughout the incubation period of up to 21 days.

Apple and Bjornson (2019) did not filter samples, and nitrifying bacteria were not inhibited. So, the amount of oxygen utilized during incubation is due to not only both autotrophic and heterotrophic respiration but also nitrification.

Field replicates serve a key purpose, not only for quantification of the variability of observations but also when comparing observations to model predictions that represent a much larger spatial area, as is the case with each of the SSM nodes. The Apple-Bjornson dataset is composed of single monthly samples at all locations except BLL040, as noted above. So, this data set can provide limited insights regarding spatial variability in the immediate area surrounding a site or the expected variability of the methodology from field replicates. Nonetheless, we can use the limited field replicate information to compute confidence intervals and compare them to predictions. The outcome of that analysis is shown in the Results section.

On the other hand, a small subset of the data (13 pairs of data points) shown in Table K-2 can be used to quantify the observational variability between years. In these cases, observations were obtained at the same location and the same month of the year but in different years. The mean percent difference between the data pairs is 62%. The percent differences between pairs range from 31% to 89%. Differences may be due to variations in oxygen, temperature, salinity gradients, or climatological drivers that also impact phytoplankton timing, growth rate, and distribution in the water column. These values represent the percent difference expected at these locations when measuring respiration rates on the same month but in different years. This is also an important observational metric, particularly in this case, since, out of necessity, we compare single observations obtained to represent a month in 2018 or 2019 with monthly mean hourly predictions for the years 2000, 2006, 2008, and 2014.

**Table K-1. Mean Conditions During Year-Round (Monthly) Sample Collection.**

Station	Depth (m)	Temperature (°C)	Salinity (psu)	Dissolved Oxygen (mg/L)
ADM001	129.6	10.3	28.3	7.1
ADM002	74.7	9.3	28.8	6.1
BLL009	15.8	10.2	28.2	7.3
BLL040	23.7	10.0	28.3	6.7
BLL040 <i>Field Replicate</i>	23.9	10.0	28.2	6.7
BUD005	16.8	12.5	27.6	7.7
CRR001	92.4	11.7	28.1	7.1
CSE001	50.7	12.1	27.8	7.5
DNA001	36.7	12.3	27.5	8.0
GOR001	168.2	11.8	28.1	7.7
NSQ002	89.5	11.8	27.9	7.4
OAK004	12.0	13.6	26.0	8.8
PSS019	90.9	10.8	27.7	5.9
PTH005	23.3	10.2	28.3	7.1
SAR003	140.5	10.6	27.6	6.0
SKG003	19.4	10.7	25.4	6.0

**Table K-2. Calculated Observed Rate and Percent Difference for Sample Pairs Collected in Different years but same Month of the Year.**

Count of Pairs	Station	Date Sampled	Observed Respiration Rate (mg O <sub>2</sub> /L/day)	Percent Rates Difference Between Years	Standard Deviation
1	BLL009	2018-10-05	0.23	76%	0.12
	BLL009	2019-10-15	0.06	—	—
2	BUD005	2018-09-07	0.21	45%	0.07
	BUD005	2019-09-09	0.11	—	—
3	BUD005	2018-10-09	0.42	48%	0.14
	BUD005	2019-10-07	0.22	—	—
4	CRR001	2018-09-07	0.14	60%	0.06
	CRR001	2019-09-09	0.05	—	—
5	CRR001	2018-10-09	0.17	72%	0.09
	CRR001	2019-10-07	0.05	—	—
6	DNA001	2018-09-07	0.25	59%	0.10
	DNA001	2019-09-09	0.10	—	—
7	DNA001	2018-10-09	0.18	69%	0.09
	DNA001	2019-10-07	0.06	—	—
8	GOR001	2018-09-07	0.16	73%	0.08
	GOR001	2019-09-09	0.04	—	—
9	GOR001	2018-10-09	0.19	89%	0.12
	GOR001	2019-10-07	0.02	—	—
10	NSQ002	2018-09-07	0.16	65%	0.07
	NSQ002	2019-09-09	0.06	—	—
11	NSQ002	2018-10-09	0.18	79%	0.10
	NSQ002	2019-10-07	0.04	—	—
12	OAK004	2018-09-07	0.24	45%	0.08
	OAK004	2019-09-09	0.13	—	—
13	OAK004	2018-10-09	0.14	31%	0.03
	OAK004	2019-10-07	0.10	—	—
Average			0.14	62%	0.09

# Analytical Approach

Since, as a result of the observational study design, all processes that consumed oxygen during the incubation were measured, here we compare those observations to the SSM overall respiration predictions (RESP). To calculate the rate of oxygen consumption, we used a classical first-order kinetics equation (Standard Methods for the Examination of Water and Wastewater 2023) for biological oxygen demand:

$$BOD_t = BOD_u (1 - e^{-kt})$$

Where:

$BOD_t$  = Biological oxygen demand at time  $t$  in  $mg\ O_2/L$

$BOD_u$  = Ultimate biological oxygen demand in  $mg\ O_2/L$  (represents the initial oxygen demand)

$k$  = rate constant (1/time)

$t$  = time (hours or days)

To calculate the two unknowns ( $BOD_u$  and  $k$ ) from the experimental data, we iterated until convergence using the nonlinear least squares function in R statistical software. Since up to four laboratory replicates were available for the same sample, we aggregated the laboratory replicates for the convergence calculations. Most (84%) of the samples (171 incubation sets out of a total of 204 field samples incubated) achieved convergence. Samples that did not achieve convergence were rejected from further analysis.

The initial rate, at the moment the sample was collected, was then calculated by multiplication of  $BOD_u$  and  $k$ . The units were converted to  $mg\ O_2/L/day$ . However, since samples were incubated at  $10^\circ C$ , and the temperatures fluctuated substantially at most locations throughout the year, we corrected the observations to the average monthly predicted temperatures at each location using the exponentially increasing temperature function employed by Cerco and Cole (1995) shown below:

$$\text{Temperature correction factor for metabolic rate} = e^{KTbx(T-T_{ref})}$$

Where:

$KTbx$  = Effect of temperature on metabolism ( $0.069/^\circ C$ )

$T$  = Temperature to be corrected to ( $^\circ C$ )

$T_{ref}$  = Reference temperature ( $10^\circ C$ )

## Results

The 2018 – 2019 Apple-Bjornson observational data set does not differentiate between respiration processes. However, since SSM tracks and predicts three oxygen-consuming processes, we compiled each of the predicted rates by monthly mean and station for the years with available SSM runs to determine the predicted contribution of each process to the overall oxygen consumption rates at the bottom layers of the water column at each observational station.

Figure K-5 shows the relative proportion of microalgal respiration (ALG\_RESP), heterotrophic respiration (DDOC), and nitrification (NITRIF) at each of the observational stations computed from the sum of hourly output for each predicted water column oxygen-consuming process over the four simulated years. Algal respiration contributes a higher proportion of the total predicted water column respiration rate at most locations. The site with the highest proportion of algal respiration (approximately 57%) is OAK004, which is also the shallowest site in this group at a depth of 12m. The site predicted to exhibit the least proportion of algal respiration (about 22%) is SAR003. This is the second-deepest site in this group at 140.5 m. SAR003 also is predicted to experience the maximum proportion of heterotrophic respiration rate (approximately 38%) and the maximum nitrification rate (approximately 41%).

Since the monthly mean observed rates for November, December, and February through August are based on single observations at each location, their representativeness in space and time is limited. Nonetheless, we conducted a comparison between monthly mean observations and measurements. Table K-3 shows the mean predicted overall rate RESP over four years of simulations (2000, 2006, 2008, and 2014) and temperature-corrected observed respiration rates collected between September 2018 and October 2019 by station. The observed rates are higher than the predicted rates. Percent differences between observed and predicted rates vary from 29% to 66%, with a mean difference of 55%. These differences are less than the percent differences between observations from different years shown in Table K-2. This result implies that the predicted respiration rates are within the expected observational ranges at these locations.

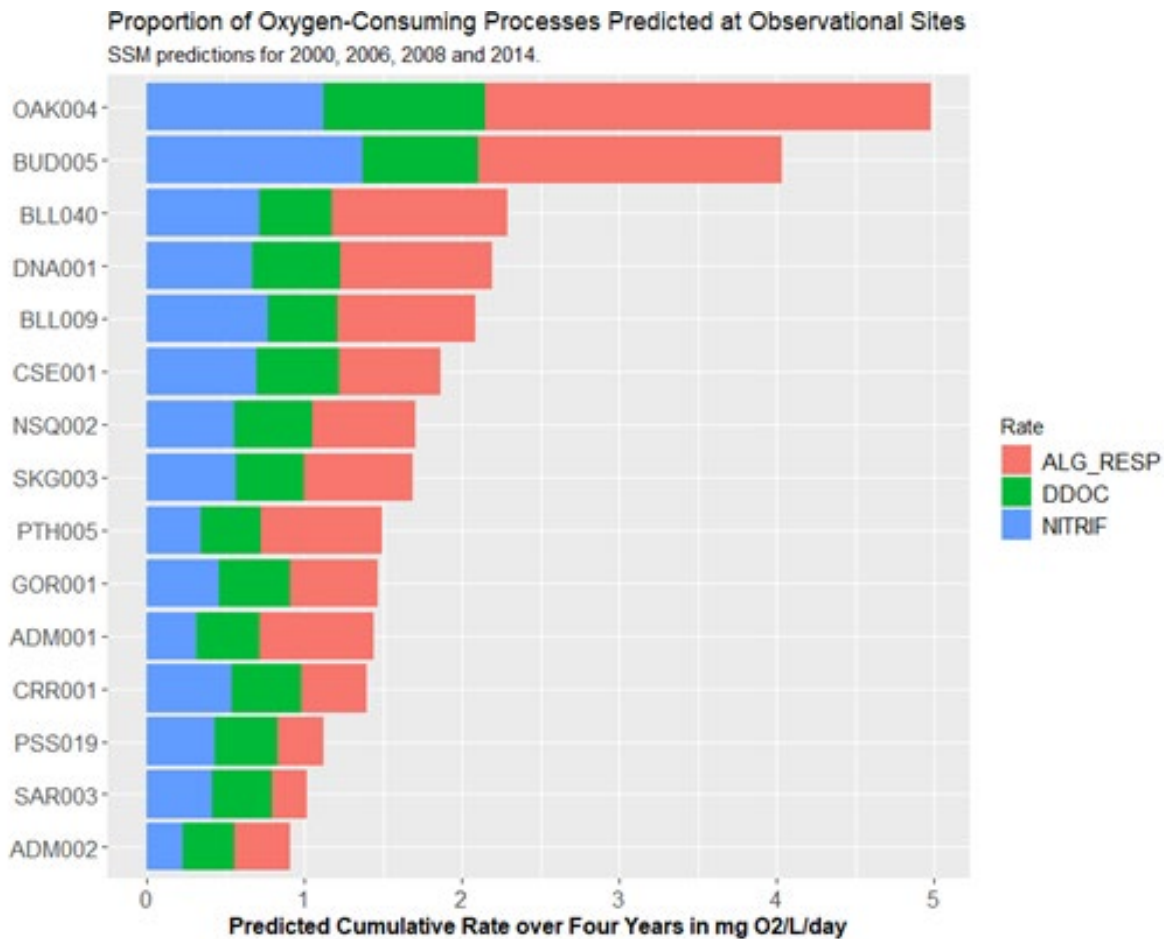


**Figure K-5. Comparison by Station of Predicted Oxygen-Consuming Processes in Bottom Waters of Observational Stations.**

Hourly predictions for each station and process are summed for the years 2000, 2006, 2008, and 2014.

Figure K-6 shows boxplots of the predicted and observed rates by the observational station. Aside from higher means, observations show a greater degree of spread beyond the interquartile range as well as multiple outliers. However, the relative pattern of the stations' order from higher rates to lower rates is very similar. Predictions and observations both show BUD005 and OAK004 with significantly higher means and spread than the other sites. The spread of the data tightens as the mean respiration rates decrease. We see coherence in the predicted and observed rates. All observed and predicted boxplots overlap at least on the high end of the predictions and the low end of the observations.

**Table K-3. Mean Predicted and Observed Respiration Rates**

<b>Station</b>	<b>Mean Predicted Rate (mg O<sub>2</sub>/L/day)</b>	<b>Mean Observed Rate (mg O<sub>2</sub>/L/day)</b>	<b>Percent Difference</b>
ADM001	0.03	0.05	45%
ADM002	0.02	0.04	57%
BLL009	0.04	0.13	66%
BLL040	0.05	0.07	29%
BUD005	0.08	0.23	64%
CRR001	0.03	0.06	55%
CSE001	0.04	0.07	48%
DNA001	0.05	0.12	62%
GOR001	0.03	0.06	52%
NSQ002	0.04	0.07	47%
OAK004	0.10	0.20	48%
PSS019	0.02	0.05	51%
PTH005	0.03	0.08	62%
SAR003	0.02	0.04	49%
SKG003	0.04	0.07	52%
Mean	0.04	0.09	55%

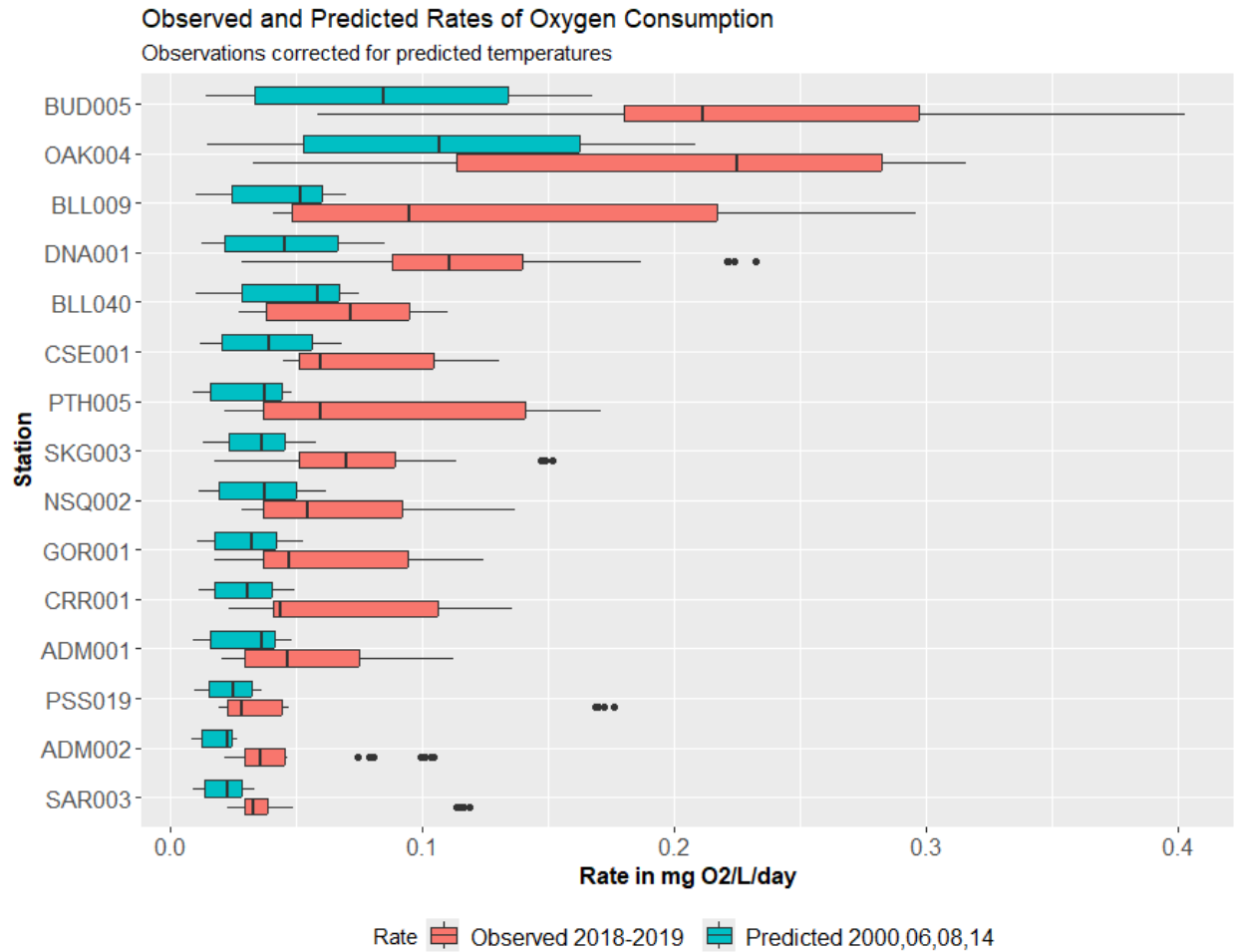


**Figure K-6. Boxplots of Observed and Predicted Respiration Rates Grouped by Observational Station.**

Observations conducted by Apple and Bjornson in 2018 and 2019 corrected to monthly mean predicted temperatures in 2000, 2006, 2008, and 2014.

Figure K-7 shows a comparison of predictions and observations grouped by month. Again, the observations show a much greater spread for each month than the predictions. Both datasets show a yearly cycle pattern, but the variability of the observations diffuses the signal in that dataset. All months resulted in overlapping boxplots for observations and predictions, except for October. October is also the month with the greatest disparity in means. The means between the two datasets are almost identical in August.

Observed and Predicted Rates of Oxygen Consumption Compared by Month Across all Stations  
 Observations corrected for predicted temperatures

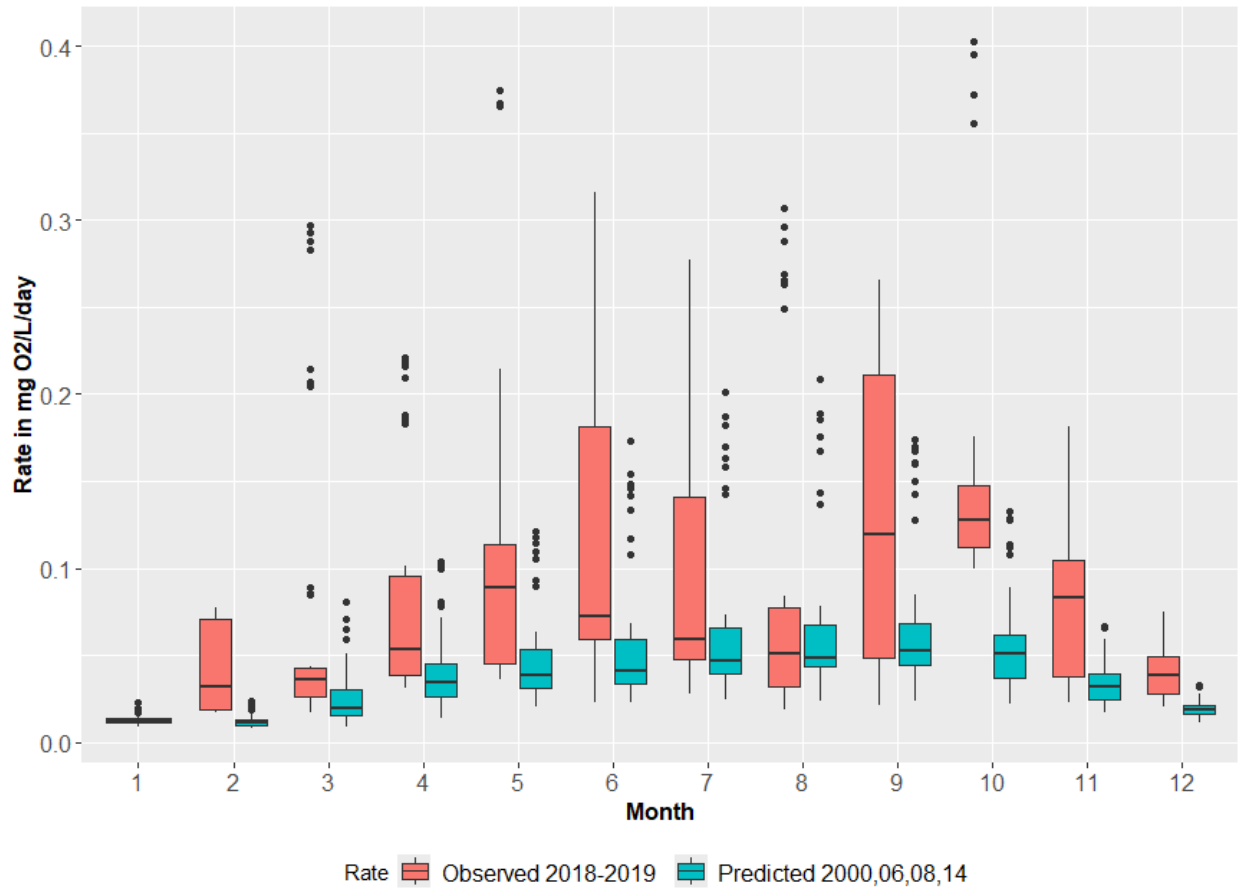


**Figure K-7. Boxplots of Observed and Predicted Respiration Rates Grouped by Month.** Predictions are for 2000, 2006, 2008, and 2014.

At only a single site, BLL040, pairs of field replicates were obtained during eight sampling events and different months. Confidence interval calculations for observed means at the same location and time are only possible for this subset of data for which field replicates were collected, and point to the variability of the observational method itself. We computed 97.5<sup>th</sup> percentile intervals (alpha=2.5%) for the observation means using the T-distribution. For the predictions, we computed normal distribution confidence intervals for the means of hourly data (for all four simulated years) within each of the eight months for which observational field replicates are available.

Figure K-8 shows the mean and 97.5<sup>th</sup> percentile confidence interval of the observed 2018 – 2019 respiration rates calculated using the T-distribution from the single pairs of sample and field replicates obtained in each of the months shown and corrected to the predicted mean temperatures of the months corresponding to the SSM model run years (2000, 2006, 2008 and 2014). In blue are the mean and 97.5<sup>th</sup> percentile confidence intervals corresponding to the predicted respiration rate (RESP) for the same four years. In May – July, the observed respiration rates were higher than the predictions, and in August, the predictions were higher

than the observations at this station. Though the observations correspond to different years, the confidence intervals overlap in March, October, November, and December.

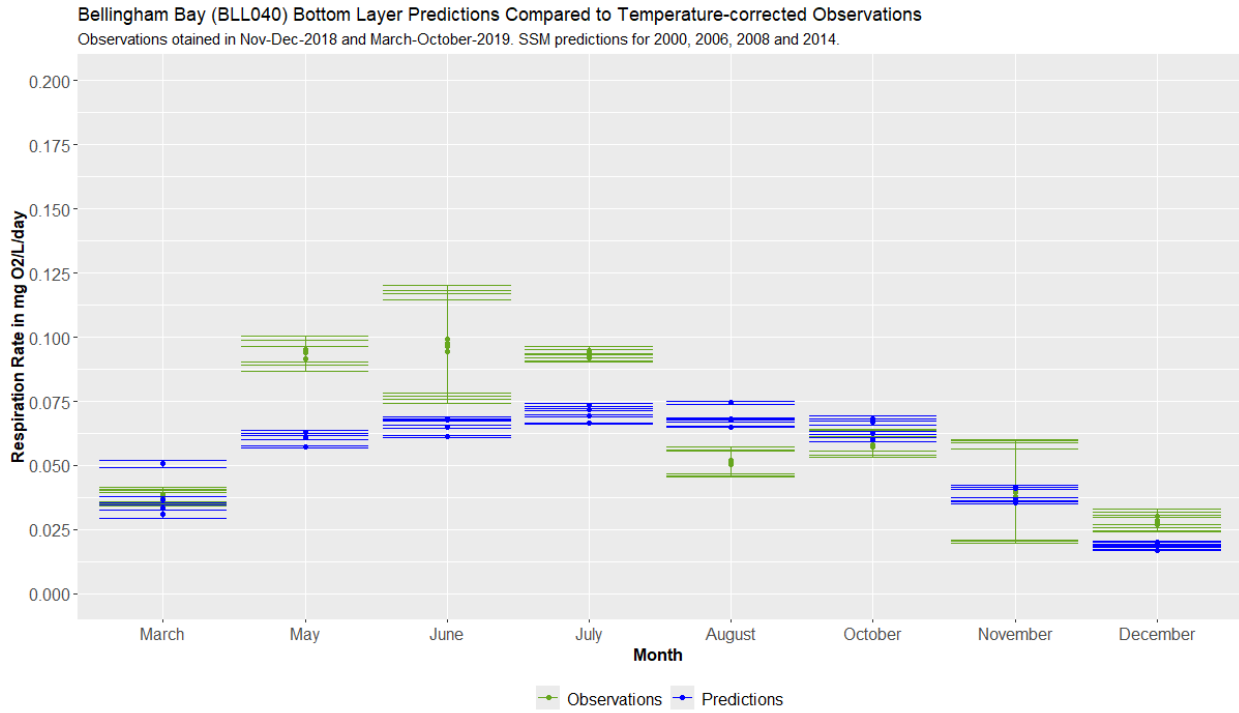


**Figure K-8. Predicted and Observed Respiration Rate Mean and Confidence Intervals for BLL040 (Bellingham Bay).** Predictions are for the years 2000, 2006, 2008, and 2014. Observations were obtained in 2018 and 2019 but corrected for monthly temperatures predicted for the above four years. Intervals are for the 97.5<sup>th</sup> percentile.

## Conclusions

Salish Sea simulations produced respiration rates that show coherent spatio-temporal patterns. Terminal inlets and bays are predicted to have higher respiration rates. Predictions also indicate an expected annual respiration cycle, with minima in the winter and maxima in the summer.

Simulations indicate that algal respiration is proportionally greater in the early spring, summer, and early fall months compared to the winter and late fall months. Heterotrophic respiration is predicted to be proportionally greater in the winter. Algal respiration is predicted to contribute the largest proportion of oxygen consumption due to water column respiration processes in the bottom waters at most of the observational stations. Heterotrophic respiration and nitrification are also present, though in smaller proportions at the locations studied.

Apple and Bjornson (2019) produced a unique observational dataset of Salish Sea microbial respiration rates for bottom waters. We compared those observations to respiration rates obtained from SSM simulations over a four-year period that did not encompass the observations. Nonetheless, we found general agreement between the observations and predictions of respiration rates at the 15 Salish Sea stations where data were collected.

Monthly mean observations were, on average, approximately 55% higher than predictions (0.09 compared to 0.04 mg O<sub>2</sub>/L/day). This difference between predictions and observations is less than the mean percent difference between observations at the same stations conducted in different years, which is 62%. Therefore, the inconsistency between the years used for simulations and those when the observations were collected may result in a bias when comparing observed and predicted values. Another factor that may bias the comparison is the value of K<sub>Tbx</sub> used in the temperature correction term. Upon considering these factors, predictions and observations are found to deviate within a reasonable and expected range.

In conclusion, predicted respiration rates are within the expected observational ranges at the sites Apple and Bjornson (2019) sampled. Furthermore, observed and predicted confidence intervals derived from field replicates obtained at a single station are in close proximity or overlap each other for most of the months for which data are available. This is another piece of evidence supporting that the observed and predicted microbial respiration datasets are representative of the same underlying processes.

## References

- Apple, J., Bjornson, S., Figueroa-Kaminsky, C., Pelletier, G. 2019. Quality Assurance Project Plan: Spatial and Seasonal Variability in Salish Sea Bottom-Water Microbial Respiration, Ecology publication 19-03-106, <https://apps.ecology.wa.gov/publications/SummaryPages/1903106.html>
- Apple, J., and Bjornson, S. 2019. Spatial and seasonal variability in Salish Sea bottom-water microbial respiration, Final Project Report. EIM Data Link: <https://apps.ecology.wa.gov/eim/search/Detail/Detail.aspx?DetailType=Study&SystemProjectId=99971985>.
- Antia, N.J. 1976. Effects of temperature on the darkness survival of marine microplanktonic algae. *Microb Ecol* 3, 41–54 <https://doi.org/10.1007/BF02011452>
- Cerco, C. F., and Cole, T. 1995. "User's guide to the CE-QUAL-ICM three-dimensional eutrophication model, release version 1.0," Technical Report EL-95-15, U.S. Army Engineer Waterways Experiment Station, Vicksburg, MS.
- Standard Methods for the Examination of Water and Wastewater. 2023. 5210 Biochemical Oxygen Demand (BOD), 24<sup>th</sup> Edition. <https://www.standardmethods.org/doi/10.2105/SMWW.2882.102>.
- Williams, P. 1981. Microbial contribution to overall marine plankton metabolism: direct measurements of respiration, *Oceanologica Acta*, 4(3), 359 – 363.